Drifting field-aligned density structures in the night-side polar cap

O. Santolík,[1,2,3] A. M. Persoon,[1] D. A. Gurnett,[1] P. M. E. Décréau,[4] J. S. Pickett,[1]
O. Maršálek,[1,2] M. Maksimovic,[5] and N. Cornilleau-Wehrlin[6]

Received 7 October 2004; revised 26 January 2005; accepted 23 February 2005; published 29 March 2005.

[1] Spatio-temporal properties of density irregularities in the night-side polar cap are inferred from multi-point observations of auroral hiss at a radial distance of 5 Earth radii. In this case study, we use high resolution data of the wave instruments onboard the four Cluster spacecraft to estimate the local plasma density, obtaining values close to 1 cm^{-3} with density depletions decreasing down to 0.15 cm^{-3}. Combined analysis in different points in space conclusively shows for the first time that these density structures are field-aligned and that they predominantly drift in the anti-sunward direction at speeds of a few km/s. This corresponds to a dawn-to-dusk convection electric field of approximately 1 mV/m. The transverse dimension of the observed density depletions, mapped down to the ionospheric heights, is of the order of a few tens of km. Their lifetime is probably longer than tens of seconds.
Citation: Santolík, O., A. M. Persoon, D. A. Gurnett, P. M. E. Décréau, J. S. Pickett, O. Maršálek, M. Maksimovic, and N. Cornilleau-Wehrlin (2005), Drifting field-aligned density structures in the night-side polar cap, *Geophys. Res. Lett.*, *32*, L06106, doi:10.1029/2004GL021696.

1. Introduction

[2] The polar cap is a low-density region of the terrestrial magnetosphere, magnetically connected to the tail lobes. Its projection along the magnetic field lines onto the Earth surface maps poleward from the auroral oval. Plasma convection in this region is believed to be controlled by the interplanetary magnetic field [e.g., *Bristow et al.*, 2004]. Auroral hiss emissions (see a review by *LaBelle and Treumann* [2002]) propagating from the auroral region to the polar cap can be used to estimate the local plasma density. Using the data of the DE-1 spacecraft, *Persoon et al.* [1983] found that the total plasma density was around 1 cm^{-3} at a radial distance (R) of 4.5 Earth radii (R_E). These results have been refined by subsequent measurements using different methods [e.g., *Johnson et al.*, 2001; *Ichikawa et al.*, 2002, and references therein]. The recent empirical model of *Nsumei et al.* [2003] is based on the radio sounding method. At the same R, this model gives average densities from 1.6 cm^{-3} (for a low geomagnetic activity) to 13 cm^{-3} (at geomagnetically disturbed times).

[3] The Cluster spacefleet passes through the polar cap region at radial distances between 5 and 13 R_E [*Vaith et al.*, 2004] and allows us to measure the local plasma density by different techniques. These multi-point measurements have an important additional potential in estimating the three-dimensional shape and motion of observed density structures.

[4] In this case study, we use the technique of *Persoon et al.* [1983] based on the measurement of the sharp upper frequency cutoff of the whistler-mode auroral hiss and we show that this technique gives a reliable estimate of the local plasma density. From a correlation analysis of density structures measured at four different spatial points we further estimate their drift velocity and size. We use high-resolution measurements of the WBD instruments [*Gurnett et al.*, 2001], independent estimations of plasma density from the WHISPER active sounders [*Décréau et al.*, 2001], and Poynting flux measurements by the STAFF-SA instruments [*Cornilleau-Wehrlin et al.*, 2003].

2. Upper Cutoff of Auroral Hiss

[5] Under the cold plasma approximation, the whistler mode has a principal resonance at the local electron cyclotron frequency (f_{ce}), or at the local plasma frequency (f_p), whichever is lower. Above this limiting frequency, the mode cannot propagate. f_{ce} can be accurately determined by onboard measurements of the magnetic field, and if we observe a sharp upper cutoff of whistler-mode hiss at a lower frequency we can use it to estimate the local f_p using the technique of *Persoon et al.* [1983]. This requires that the whistler-mode waves propagate in the direction of decreasing f_p, which, in the inner magnetosphere, means outward from the Earth.

[6] An example of such data was recorded on March 11, 2002 by the wave instruments on board the four Cluster spacecraft. An intense emission of auroral hiss was observed between 0805 and 0905 UT. The emission had a characteristic funnel-shaped lower-frequency cutoff usually attributed to propagation from a source localized in the auroral region [*Gurnett et al.*, 1983]. As the spacecraft moved from the auroral zone to the Northern polar cap after 0830 UT, a sharp upper cutoff was observed well below the measured f_{ce}. Figure 1 shows a small subset of these high-resolution measurements from Cluster 1 and Cluster 4. The time-frequency power spectrograms of the electric field fluctuations measured by the WBD instruments reflect the modulation of the signal by the spacecraft spin with a period of 2 s (one half of the spin period). This

[1]Department of Physics and Astronomy, University of Iowa, Iowa City, Iowa, USA.
[2]Permanently at Faculty of Mathematics and Physics, Charles University, Prague, Czech Republic.
[3]Also at IAP/CAS, Prague, Czech Republic.
[4]LPCE/CNRS, Orleans, France.
[5]LESIA, Observatoire de Paris, Meudon, France.
[6]CETP/IPSL, Velizy, France.

0094-8276/05/2004GL021696$05.00

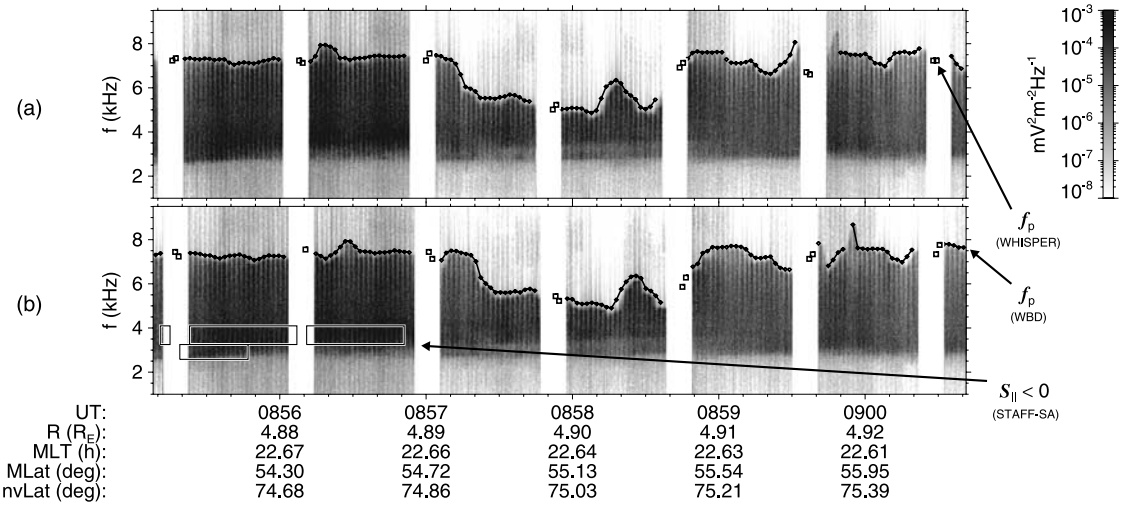

Figure 1. Example of high resolution multipoint measurements recorded on March 11, 2002 on board (a) Cluster 1, and (b) Cluster 4. Time-frequency power spectrograms of electric field fluctuations from the WBD instruments are over-plotted by line-connected solid symbols showing an estimate of the local plasma frequency (f_p) from these measurements. Open square symbols represent f_p determined using the data of the WHISPER active sounder. Rectangles show time and frequency intervals where analysis of measurements of the STAFF-SA instrument gives a significant antiparallel component of the Poynting flux. Position is given on the bottom: R-radial distance; MLT-magnetic local time; MLat-magnetic latitude; InvLat-invariant latitude calculated from a simple geocentric dipolar model. The local f_{ce} is 13.4–13.7 kHz (not shown).

modulation is expected for waves propagating close to the whistler-mode resonance cone. Periodic electric-field data gaps occur on the spectrogram when WBD is switched to measure the magnetic field fluctuations in the time intervals closely surrounding the active measurements of the WHISPER sounder.

[7] At $R \sim 4.9\ R_E$, where the measurements took place, we expect upward propagation of auroral hiss with a component antiparallel to the magnetic field direction in the Northern polar cap [*Santolík and Gurnett*, 2002]. Indeed, the parallel component of the Poynting flux ($S_{||}$), as derived from the data of the STAFF-SA instrument, is significantly negative (i.e., antiparallel) between 0816–0828 UT, as the four spacecraft passed over the auroral hiss source. Significantly negative $S_{||}$ also occurs inside regions shown by horizontal rectangles in the time-frequency plane in Figure 1b. These regions are limited by intervals when the magnetic field fluctuations are measurable and when hiss occurs below the upper frequency limit of the STAFF-SA instrument (4 kHz).

[8] The upper cutoff is detected by an automated procedure based on the individual power spectra from the WBD instrument. The results are plotted over the time-frequency spectrograms in Figure 1. Their interpretation as the local f_p is validated by independent measurements of the WHISPER active sounder. f_p estimated from the sounder data using the method of *Trotignon et al.* [2001] generally agrees well with the upper cutoff seen in the neighboring WBD spectra. The underlying density variations are also reflected by the changes of the spacecraft potential measured by the Electric Field and Wave Experiment (EFW) instrument onboard the Cluster spacecraft (A. Vaivads, private communication, 2004).

[9] During the entire pass through the polar cap, the f_p values obtained from the WBD spectra correspond the density varying from 0.6 to 1.2 cm^{-3} with density depletions decreasing down to 0.15 cm^{-3}. The observed density in the analyzed case is slightly below the model of *Nsumei et al.* [2003] which gives a value of 1.51 cm^{-3} for the Kp index of 2^- obtained in the 3-hour period preceding the event.

3. Multi-point Analysis of Density Fluctuations

[10] Figure 1 indicates that temporal variations of f_p observed on Cluster 1 are well correlated with the results obtained on Cluster 4, but a time lag of ≈10 s is apparent. To quantify the correlation coefficient and the optimum time lag we have calculated the Spearman's rank correlation coefficient ρ [e.g., *Press et al.*, 1992] of the plasma density estimates corresponding to the time series of the obtained f_p values. Since the time resolution of the f_p estimates is 2 s, we have varied the time lags with 2-s increments. We have used those data points where an f_p estimate was obtained at a given time t from Cluster 4, and an f_p estimate was also obtained from Cluster 1 at a lagged time $t + \tau$. This means that the electric-field data gaps seen in Figure 1 were not interpolated and only those density values which directly correspond to existing upper-cutoff (f_p) estimates were used.

[11] Similar calculation has then been done using the data from each of the six possible pairs of the four spacecraft. Figure 2 shows examples of the results for two spacecraft pairs in the time interval from 0856 to 0900 UT (see Figure 1). Correlation of Cluster 1 and 4 gives the maximum value of $\rho = 0.98$ (the largest between the six pairs) for a distinct peak centered at a time lag $\tau_* = +9$ s (Figure 2a). Similarly, for correlation of Cluster 3 and 4, the maximum of $\rho = 0.84$ (the smallest between the six pairs) is found for a peak centered at $\tau_* = -22$ s (Figure 2b). Both maxima are statistically significant, well beyond the level of one stan-

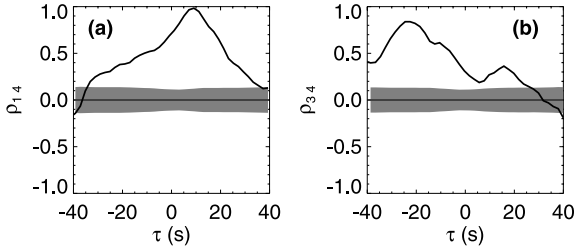

Figure 2. Spearman's rank correlation coefficient as a function of time lag between the two time series of density estimates obtained from (a) Cluster 1 and Cluster 4; (b) Cluster 3 and Cluster 4. Data were processed in the time interval from 0856 to 0900 UT (see Figure 1). Shaded areas show one-σ_ρ levels for the correlation coefficient of a hypothetical set of uncorrelated data.

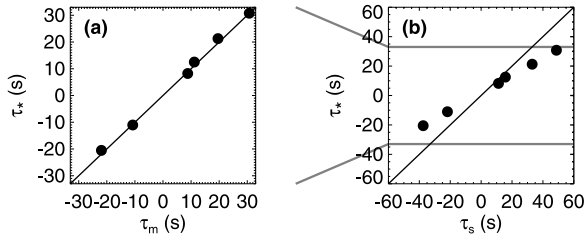

Figure 3. Time lags τ_* corresponding to the largest peaks in the rank correlation coefficient ρ versus (a) theoretical time lags τ_m supposing drifting density structures; (b) theoretical time lags τ_s supposing stationary field-aligned density structures (see text). The data were obtained from the six spacecraft pairs in the time interval between 0856 and 0900 UT (see Figure 1).

dard deviation (σ_ρ) which would correspond to an absolutely uncorrelated data set of the same size as the real data.

[12] The six optimum time lags from the entire set of spacecraft pairs can be used to investigate the 3D properties of the underlying density irregularities, similarly as it was described for ground-based observations of the ionosphere by *Briggs et al.* [1950]. We will use a model involving a proper motion of a density structure with a speed u along its normal direction ($\hat{\mathbf{n}}$), supposing for simplicity that the irregularities do not evolve in time during their encounter with the spacecraft. Seen from moving spacecraft, this proper motion is superposed over the orbital velocity ($\mathbf{v_s}$).

[13] For a known separation vector ($\mathbf{q}$) of two given spacecraft ($|\mathbf{q}|$ is, in this case, between 90 and 225 km), we can calculate the theoretical time delay, $\tau_m = \mathbf{q} \cdot \hat{\mathbf{n}}/(u - \mathbf{v_s} \cdot \hat{\mathbf{n}})$. The free parameters are the speed u, and the local normal direction $\hat{\mathbf{n}}$. To express this direction we will use a field-aligned coordinate system with the $\hat{\mathbf{e}}_\mathbf{b}$ axis along the ambient magnetic field $\mathbf{B_0}$, the "sunward" $\hat{\mathbf{e}}_\mathbf{s}$ axis obtained from $\mathbf{B_0} \times \hat{\mathbf{y}}_\mathbf{GSE}$, and the "duskward" axis $\hat{\mathbf{e}}_\mathbf{d} = \hat{\mathbf{e}}_\mathbf{s} \times \hat{\mathbf{e}}_\mathbf{b}$ [see *Vaith et al.*, 2004].

[14] The normal direction $\hat{\mathbf{n}}$ can be generally defined by two spherical angles: a cone angle (θ) measured from the $\hat{\mathbf{e}}_\mathbf{b}$ axis and an azimuth-clock angle (α) measured from the $\hat{\mathbf{e}}_\mathbf{s}$ axis in the $\hat{\mathbf{e}}_\mathbf{d} - \hat{\mathbf{e}}_\mathbf{s}$ plane, i. e., in the plane perpendicular to $\mathbf{B_0}$. Parameters α, θ, and u can be optimized by a nonlinear least squares method to obtain the six theoretical time delays τ_m as close as possible to the six measured delays τ_*.

[15] For the interval 0856–0900 UT, this procedure leads to a good agreement between the measured and theoretical time delays (see Figure 3a), yielding $\alpha = 163°$, $\theta = 96°$, and $u = 2.7$ km/s. The obtained values mean that the density structure is field-aligned ($\hat{\mathbf{n}}$ is close to perpendicular to $\mathbf{B_0}$), and that it moves along $\hat{\mathbf{n}}$ approximately in the anti-sunward direction. Figure 1 shows that the major density irregularity in this particular interval is a depletion traversed by Cluster 1 between 0857:15 and 0858:47. The observed motion of the density structure (superposed over the spacecraft orbital velocity) gives us an estimate of the linear dimension of the depletion of ≈650 km measured parallel to its normal direction.

[16] For comparison, Figure 3b shows the results for a simple model of stationary field-aligned structures with a single free parameter α. The proper motion of the structures is here supposed to be negligible with respect to the orbital speed of the spacecraft (≈4.5 km/s). In that case, the observed time lags would be solely attributed to the orbital velocity of the spacecraft passing successively through a density structure. It is evident that the optimized theoretical time delays τ_s are considerably longer than the observed ones. This clearly shows that a model of drifting structures is necessary to explain the observations.

4. Correlation Analysis of Several Time Intervals

[17] Similar analysis has been done for 7 time intervals throughout the polar cap pass on March 11, 2002, between 0834 and 0905 UT. Duration of these intervals was always 4 minutes to ensure a reasonable statistical significance of the correlation coefficients, with maxima well beyond the one-σ_ρ levels for the correlation coefficient of a hypothetical set of uncorrelated data. All those cases were located on the nightside between 2256 and 2234 MLT and the radial distances varied from 4.7 to 5 R_E.

[18] Figure 4 shows the obtained normal directions as a function of the invariant latitude calculated from the central spacecraft positions using a simple dipole model. The results indicate that all the observed density structures can be considered as field-aligned since θ is always close to 90° (Figure 4a). The results for α (Figure 4b) show prevailing anti-sunward orientation of the local normal, especially at higher invariant latitudes. Resulting values of u give speeds

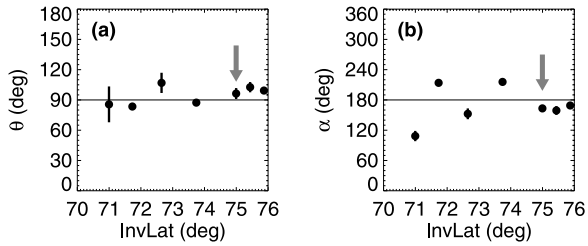

Figure 4. Two angles defining the normal direction of moving density structures as a function of the invariant latitude. (a) Angle deviation θ from the ambient magnetic field. (b) Angle azimuth α measured from the "sunward" $\hat{\mathbf{e}}_\mathbf{s}$ axis of the field-aligned coordinate system. Error bars indicate standard deviations estimated from the parameter optimization procedure. Grey vertical arrows show the results obtained from the example interval in Figure 1.

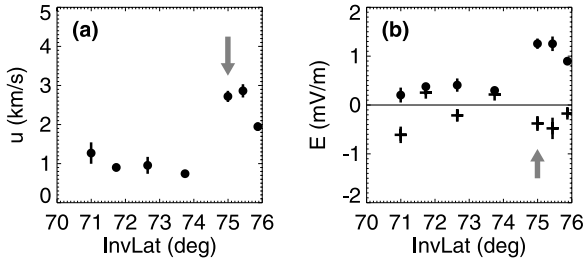

Figure 5. Convection parameters of density structures as a function of the invariant latitude. (a) Convection speed u. (b) Convection electric field $\mathbf{B_0} \times \mathbf{u}$; plus signs: "sunward" E_s component; solid circles: "duskward" E_d component.

of 1 km/s, increasing to 2–3 km/s at higher latitudes (Figure 5a). Since the irregularities are assumed to move along their local normal directions, their velocity is mainly oriented perpendicular to the magnetic field lines and antisunward. This magnitude and direction of the drift motion is roughly consistent with the simultaneous measurements of the Electron Drift Instrument (EDI) instrument onboard the Cluster spacecraft (G. Paschmann, private communication, 2004) but a detailed comparison is beyond the scope of this letter.

[19] Figure 5b shows the convection electric field obtained from these velocities as $\mathbf{E} = \mathbf{B_0} \times \mathbf{u}$. The "sunward" E_s component is most often negative with absolute values below 0.6 mV/m, while the "duskward" E_d component is consistently positive, increasing from 0.3 mV/m to 1.3 mV/m at higher latitudes. These values, using an estimated diameter of 6 R_E for the polar cap at a radial distance of 5 R_E, give a rough estimate of the cross-polar cap potential of 50 kV which is close to the average potential drop observed by ground-based radars [*Bristow et al.*, 2004]. For the particular time interval considered in the present letter, provisional SuperDARN estimations of the cross-polar cap potential are between 40 and 50 kV. The propagation-delay shifted interplanetary magnetic field (IMF), as measured in the upstream solar wind by the ACE spacecraft, shows first a southward B_Z (in the GSM frame) component and a dawnward B_Y component of approximately the same strength. Later, when the Cluster spacecraft moves to invariant latitudes above 75° where we observe an abrupt change of the convection speed (see Figure 5a), the IMF B_Z component nearly disappears, while B_Y still is dawnward, diminishing and becoming slightly duskward just before the end of the investigated time interval.

[20] The major density irregularities in this data set were depletions in which the spacecraft spent between 30 and 100 s. These durations, combined with the obtained convection velocities between 0.7 and 2.9 km/s and the spacecraft orbital velocities of 4.5–4.6 km/s, result in linear dimensions of those depletions from 100 to 650 km parallel to their normals. Mapped along the magnetic field lines to the ionosphere these dimensions scale down to ≈9–60 km.

[21] Analysis of the cross-spacecraft correlation can give us more information about the shape and characteristic time scales of the observed density structures. On average, the obtained values of the maximum correlation coefficient seem to decrease only slightly as a function of the time lag between the spacecraft, which means that the average lifetime of the density structures is probably higher than tens of seconds. Similarly, the correlation coefficient does not substantially decrease with the separation of the spacecraft perpendicular to the normal direction at scales up to 200 km, although some decrease could be noted. A refined analysis for different separation scales is needed.

[22] **Acknowledgments.** We thank G. Paschmann for providing the EDI data, A. Vaivads for providing the EFW data (PI M. André), and the international network SuperDARN for providing the convection maps at http://superdarn.jhuapl.edu. We acknowledge the access to the spin-resolution FGM data (PI A. Balogh) used for reference. We thank the MAG and SWEPAM teams and the CDAWeb for providing the ACE data. This research was supported by the NASA Goddard Space Flight Center under Grants No. NAG5-9974 and NNG04GB98G, and by the NSF award No. 0307319/ME 650. O. Santolík acknowledges additional support from grant GACR 202/03/0832.

References

Briggs, B. H., G. J. Phillips, and D. H. Shinn (1950), The analysis of observations on spaced receivers of the fading of radio signals, *Proc. Phys. Soc. B*, *63*, 106–121.

Bristow, W. A., R. A. Greenwald, S. G. Shepherd, and J. M. Hughes (2004), On the observed variability of the cross-polar cap potential, *J. Geophys. Res.*, *109*(A2), A02203, doi:10.1029/2003JA010206.

Cornilleau-Wehrlin, N., et al. (2003), First results obtained by the Cluster STAFF experiment, *Ann. Geophys.*, *21*, 437–456.

Décréau, P. M. E., et al. (2001), Early results from the Whisper instrument on Cluster: An overview, *Ann. Geophys.*, *19*, 1241–1258.

Gurnett, D. A., S. D. Shawhan, and R. R. Shaw (1983), Auroral hiss, Z mode radiation, and auroral kilometric radiation in the polar magnetosphere: DE 1 observations, *J. Geophys. Res.*, *88*, 329–340.

Gurnett, D. A., et al. (2001), First results from the Cluster wideband plasma wave investigation, *Ann. Geophys.*, *19*, 1259–1272.

Ichikawa, Y., T. Abe, and A. W. Yau (2002), Plasma density enhancements in the high-altitude polar cap region observed on Akebono, *Geophys. Res. Lett.*, *29*(9), 1327, doi:10.1029/2001GL013723.

Johnson, M. T., J. R. Wygant, C. Cattell, F. S. Mozer, M. Temerin, and J. Scudder (2001), Observations of the seasonal dependence of the thermal plasma density in the Southern Hemisphere auroral zone and polar cap at 1 R_E, *J. Geophys. Res.*, *106*, 19,023–19,033.

LaBelle, J., and R. A. Treumann (2002), Auroral radio emissions, 1. Hisses, roars, and bursts, *Space Sci. Rev.*, *101*, 295–440.

Nsumei, P. A., X. Huang, B. W. Reinisch, P. Song, V. M. Vasyliunas, J. L. Green, S. F. Fung, R. F. Benson, and D. L. Gallagher (2003), Electron density distribution over the northern polar region deduced from IMAGE/radio plasma imager sounding, *J. Geophys. Res.*, *108*(A2), 1078, doi:10.1029/2002JA009616.

Persoon, A. M., D. A. Gurnett, and S. D. Shawhan (1983), Polar cap electron densities from DE 1 plasma wave observations, *J. Geophys. Res.*, *88*, 10,123–10,136.

Press, W. H., B. P. Flannery, S. A. Teukolsky, and W. T. Vetterling (1992), *Numerical Recipes*, Cambridge Univ. Press, New York.

Santolík, O., and D. A. Gurnett (2002), Propagation of auroral hiss at high altitudes, *Geophys. Res. Lett.*, *29*(10), 1481, doi:10.1029/2001GL013666.

Trotignon, J. G., et al. (2001), How to determine the thermal electron density and the magnetic field strength from the CLUSTER/WHISPER observations around the Earth, *Ann. Geophys.*, *19*, 1711–1720.

Vaith, H., et al. (2004), Plasma convection across the polar cap, plasma mantle and cusp: Cluster EDI observations, *Ann. Geophys.*, *22*, 2451–2461.

N. Cornilleau-Wehrlin, CETP/IPSL, 10/12 Avenue de L'Europe, F-78140 Velizy, France.

P. M. E. Décréau, LPCE/CNRS, 3A Avenue de la Recherche, F-45071 Orléans, France.

D. A. Gurnett, A. M. Persoon, and J. S. Pickett, Department of Physics and Astronomy, University of Iowa, Iowa City, IA 52242-1479, USA.

M. Maksimovic, LESIA, Observatoire de Paris-Meudon, Place Jules Janssen, F-92195 Meudon, France.

O. Maršálek and O. Santolík, Faculty of Mathematics and Physics, Charles University, V Holešovičkách 2, CZ-18000 Praha 8, Czech Republic. (ondrej.santolik@mff.cuni.cz)